Characterization of the local instability in the Hénon-Heiles Hamiltonian

Juan C. Vallejo, Jacobo Aguirre, and Miguel A.F. Sanjuán

Nonlinear Dynamics and Chaos Group,

Departamento de Ciencias Experimentales e Ingeniería,

Universidad Rey Juan Carlos, Tulipán s/n, 28933 Móstoles, Madrid, Spain

(Dated: April 8, 2002)

Abstract

Several prototypical distributions of finite-time Lyapunov exponents have been computed in the two-dimensional Hénon-Heiles Hamiltonian flow. Different shapes are obtained for each dynamical state. Even when an evolution is observed in the morphology of the distributions for the smallest integration intervals, they can still serve for characterizing the dynamical state of the system.

PACS numbers: 05.45.-a

I.   INTRODUCTION

Lyapunov exponents are a well known diagnostic tool for analyzing chaotic motion. In the past few years major attention has been paid in the distribution of the so called finite-time Lyapunov exponents. As the shapes of these distributions can serve as indicators of the overall degree of instability of a system, its evolution or stationarity is a key question. Our work focus in the study of the distributions calculated with the smallest time interval available, in order to see if they are still valid indicators, with such local information. The paper structure is as follows. First, we will review the different definitions found in the literature, in order to clarify many different but related concepts. Then, a set of protypical distributions for several orbit types in the Hénon-Heiles Hamiltonian will be shown. This conservative system has been selected, because in spite of its simplicity, it shows a large richness concerning the behavior of its orbits. Finally, we will end with some concluding remarks.

A.   Lyapunov Exponents

The ordinary (or global) Lyapunov exponent describes the evolution in time of the distance $z(t)$ between two nearly initial conditions, and it is defined in the following manner

$$\chi = \lim_{t \to \infty} \lim_{\delta z(0) \to 0} \frac{1}{t} \log \frac{\delta z(t)}{\delta z(0)}. \tag{1}$$

The global Lyapunov exponents have been proven to be a quite useful tool for analyzing chaotic motion, and their utility comes in part from the fact that their values do not depend upon the metric. However, since in practice the calculation is performed numerically, only a finite integration time is used instead of the infinite time defined above. This leads to an approximated value instead of the real one, producing the so-called local (or finite-time) Lyapunov exponent. This is of course more important when working with experimental data, because of the very small number of measurements.

It should be noted that neither the notation nor the definitions are standard in the literature. Since this can produce some confusion, it would be worthy to summarize some of them. Some authors as [1] and [2] use the widely found terms short-time Lyapunov characteristic numbers or local Lyapunov exponents as follows

$$\chi(\Delta t) = \lim_{\delta z(0) \to 0} \frac{1}{\Delta t} \log \frac{\delta z(\Delta t)}{\delta z(0)} \tag{2}$$

This quantity also appears later referred by these authors as (maximal) short-time Lyapunov exponent or finite-time Lyapunov exponent. Obviously the relation between them is

$$\chi = \lim_{\Delta t \to \infty} \chi(\Delta t). \tag{3}$$

Another widely used term is the Lyapunov characteristic number defined for instance in [3, 4] as

$$\chi = \lim_{t \to \infty} \frac{1}{t} \log \frac{\delta z(t)}{\delta z(0)}. \tag{4}$$

Note that this is not "short" in the sense that the deviation $\delta z(0)$ is not taken as an infinitesimal. The concept of local Lyapunov exponent or effective Lyapunov exponent appears defined in Ref. [5] as

$$\Lambda(t) = \frac{1}{t} \ln \frac{\delta z(t)}{\delta z(0)}, \tag{5}$$

and the notion of stretching number, or generalized Lyapunov indicator appears as a particular case from it when $t = 1$. Consequently the short-time Lyapunov exponent is then defined as just the stretching number divided by Δt. These definitions are strongly related to the way in which the exponents are obtained. For the computation of the exponents, we examine the length evolution of the axes of an ellipsoid defined by a set of orthonormal D-dimensional vectors centered in an initial condition. The so-called stretch exponents, following Refs. [6, 7], are the logarithms of the average growth rate per iteration (also called Lyapunov number) by which the vectors expand along the D directions. The sum of the stretch exponents after N steps divided by N is the finite-time or local Lyapunov exponent and the limit of such sum when N goes to ∞ is the global Lyapunov exponent. Details concerning the computation of the Lyapunov exponents may be found in Ref. [8]. The initial orientation of the axes leads to different effective growth rates and, in consequence, following Ref.[9], the Local Lyapunov exponents can be divided in two types: the finite-time Lyapunov exponents and the finite-sample Lyapunov exponents. The set of orthogonal vectors undergoes a few transient steps as their initial directions were chosen at random.

After a few steps of integration and orthonormalization, they might be considered already locally characteristic (that means specific of a certain local flow). So the first type refers to the case when the directions coincide with the right singular vectors of the matrix resulting from the jacobian product, and the second one, to the case when they correspond to the vectors resulting from the evolution of those singular vectors some steps before starting the computations.

B. Lyapunov Exponents distributions

If we make a partition of the whole integration time along one orbit into a series of time intervals of size Δt, then it is possible to compute the finite-time Lyapunov exponents $\chi(\Delta t)$ for each interval, and to plot the resulting distribution of values. By examining such spectrum, we can get information about the overall degree of instability of the orbit. Such an approach has proved to be useful in several fields such as galactic dynamics [10, 11], analyzing chaotic fluid flows in the context of fast dynamos [12] or chaotic packet mixing and transport in wave systems [13]. The mean of the distribution correlates with the maximal Lyapunov characteristic number, and the shape of such distribution can serve as a valid chaoticity indicator, as it shows the range of values for χ. In principle, the shape depends on the initial condition (so on the invariant measure towards it evolves), and also on the sampling interval size Δt. The distribution of finite-time Lyapunov exponents can be normalized dividing it by the total number of intervals thus obtaining a probability density function $P(\chi)$, that gives the probability of getting a given value χ between $[\chi, \chi + d\chi]$. Hence, the probability of getting a positive $\chi(\Delta t)$ or F_+ (and analogously F_-) can be defined as

$$F_+ = \int_0^\infty P(\chi)d\chi. \tag{6}$$

Two ways for calculating such distributions are possible. The first one is starting from a given initial condition and integrating during the interval Δt, thus leading to a $\chi(\Delta t)$, and starting again the cycle from that point. The second way is taking an ensemble of initial conditions on the available phase space. For each initial point, $\chi(\Delta t)$ is calculated as before, without later progression in that orbit (see for instance Refs. [1, 2, 14]). When the phase space is largely stochastic and the regular regions small, both distributions coincide, in agreement with the ergodic theorem. When regular orbits appear, they can differ

4

substantially.

C. Distribution behavior at very short-times.

We are carrying out a search on how to characterize the most chaotic orbits in a given flow. As the shapes of these distributions can serve as a valid indicator, its evolution or stationarity is a key question. This paper follows some of the ideas started in [1, 2], where the dependency on the sampling time and the evolution towards an invariant measure in the distributions from orbits in chaotic domains have been analyzed. A clear description of how these spectra characterize the dynamical state in a set of hamiltonian prototypical cases was a motivation for our work. Many distributions belonging to typical maps have been studied, as, for instance, in [7, 15, 16], but less consideration has been given to conservative systems, where no attractors are found. Indeed, we are interested in the distributions for characterizing not only the possible final invariant measure, if so, but also the orbit stability itself, including the unstable and the open orbits (those that will escape towards the infinite). The main goal will be then to generate a set of protypical distributions for those different orbit behaviors.

Several criteria for choosing a small Δt are found in the literature. The shortest interval that can be used in the case of maps is one iteration of the map. However for flows, as this time interval is a continuous quantity, several approaches are possible. It can be taken very small, although obviously not smaller than the integration step. It has not been completely established yet whether these finite-time Lyapunov exponents distributions are typical or stationary when computed with short intervals Δt ([6]).

We are interested in analyzing how the distributions calculated with the smallest available Δt interval characterize the system. Even when some variability is expected when taken such intervals, they can still serve for tracing the system. In fact, a way to determining the structure of a Lyapunov spectrum locally, that is, within some small (in principle infinitesimal) time interval is showed in Ref. [17]. Taking the interval size as small as possible, the correlation of each value to the following one will depend only on the local orbit behavior. We will try to find out if the local information is enough for obtaining valid results or we should increase such interval. Alternatively, the size can be equal to any time interval with physical meaning, such as the characteristic time of the system or the crossing time of the

orbit with a given Poincaré section. Finally, instead of a fixed Δt, it is possible to choose a variable sampling interval, as in [4], where it is taken to be equal to the interval where the $\chi(\Delta t)$ reaches a temporary limit. On the other hand, when the size of Δt is increased, the local details are washed out. In the limit, $\chi(\Delta t \to \infty)$ tends to the global Lyapunov exponent, and the distribution tends to be a Dirac-δ centered at this global value.

II. BEHAVIOR IN A TWO-DIMENSIONAL HAMILTONIAN: THE HÉNON-HEILES SYSTEM

In order to analyze distributions of finite-time Lyapunov exponents with such an approach, we have chosen the Hénon-Heiles Hamiltonian, which is a two-dimensional time independent Hamiltonian system which was originated as a model in galactic dynamics [18]. The equation of this Hamiltonian is given by

$$H = \frac{1}{2}(p_x^2 + p_y^2) + \frac{1}{2}(x^2 + y^2 + 2x^2 y + \frac{2}{3}y^3). \tag{7}$$

We are interested in this model because it is connected to a physical problem and also because in spite of its simplicity it presents a rather rich complex dynamics. According to the energy of the orbit, which is related to the initial condition, different dynamic behaviors may appear and paradigmatic examples of the so-called pseudodeterministic models can be found. These models only yield to relevant information over trajectories of reasonable length due to the unstable dimension variability (see [19, 20]). The oscillating behavior of the finite-time Lyapunov exponents about zero has been found to be associated to these models [16]. As we are dealing with a two-dimensional system, four Lyapunov exponents will exist. However, since it is a conservative Hamiltonian system, $\lambda_i = -\lambda_{5-i}$ for $(i = 1, ..., 4)$ and only two different values of λ are independent. One of them will be tangent to the trajectory, parallel to the velocity field, and the other one, transverse to it. The tangent one is non-relevant as it tends to zero in the limit case.

The distribution of the finite-time Lyapunov exponents was carried out by using standard methods, and the initial ellipse axes were chosen at random. We have used a sixth-order Runge-Kutta integrator with a fixed time step equal to 10^{-2}, because it provides enough accuracy for our purposes. And also we have carefully checked that $\lambda_i = -\lambda_{5-i}$ as the integration was evolving in time to assure the goodness of the numerical computations. The

6

Poincaré cross section with the plane $x = 0$ has been plotted for each state, in order to compare the distribution with the dynamical state. We have selected this plane because of the symmetry of the system with respect to it, so each orbit must repeatedly intersect it. Then, the crossing time is defined as the time between successive section crosses. We have started the analysis computing periodic and quasiperiodic cases. In a fully stable periodic motion, as the harmonic oscillator, when calculating the finite-time Lyapunov exponents we get a single peaked distribution centered in a given positive value, as we get the same $\chi(\Delta)$ for every interval. If the interval size increases, $\chi(\Delta t >>) \rightarrow 0$, and the peak shifts towards zero. We can compare the former case with an orbit near an Unstable Periodic Orbit (UPO). This can be observed when the energy E takes the value $1/4$, in the Lyapunov Orbit. This orbit defines a frontier. Every orbit with an initial energy larger than the escape energy and moving outwards, if it crosses the Lyapunov Orbit, will escape from the system and will never come back (see [21]). The phase space of an example of such orbit is plotted in Fig. 1(a). In an UPO, each point must avoid all regions $\chi(\Delta) < 0$. The distribution of finite-time Lyapunov exponents is formed by two peaks, both centered around positive values. When the initial condition is slightly different from the one leading to the unstable periodic orbit, the distribution is similar to the solid line of Fig. 1(b), where we observe two broadened peaks centered around positive values, and a tail associated to the orbit once it has escaped. For orbits with smaller escape times, the spectrum is different due to this tail, but while the orbit is confined, the shape is quite similar. If the interval size Δt is increased, but smaller than the escaping time, it is observed that the main peaks shift towards larger positive values and begin to merge, as shown by the dashed and dotted points of Fig. 1(b).

The following case analyzed is a quasi-periodic orbit, found in the Hénon-Heiles system for the energy $E = 1/8$. Its Poincaré surface cross section is depicted in Fig. 2(a), and it shows a set of ten islands, which is associated to a period-5 orbit. The five islands on the left are plotted when the $x = 0$ plane is crossed from the $x < 0$ subspace towards $x > 0$, and the other five on the right when returning to the $x < 0$ subspace. The distribution of finite-time Lyapunov exponents for an interval Δt of 0.02 and total integration time of 10^4 is the solid line in Fig. 2(b). It shows ten peaks, five centered around negative values and the other five centered around positive values. This means that there are arbitrarily finite intervals for which the orbit, on the average, is repelling in one of the dimensions and other intervals for which is attracting in the same dimension. The shape of the distribution

7

is independent of the initial condition along the orbit, and longer integrations do not lead to different shapes. When the initial condition is moved far away from the periodic orbit, the distribution broadens but remains with a similar morphology. When the interval size increases, the range of values around which the peaks are centered is reduced and it is shifted towards positive values, as shown in Fig. 2(b) as dotted lines. When $\Delta t = 10$, a multipeaked distribution is still observed, since this value is larger than the crossing time but smaller than the total circuit time, which is roughly 32 time units. For larger size of time intervals the peaks begin to merge, as Δt begins to be equal to that time. This behavior is different for orbits with stronger chaoticity. One example appears in Fig. 3(a), with initial energy $E = 1/12$. The solid line in Figure 3(b) shows the corresponding distribution with an integration time of 20000 units, and $\Delta t = 0.02$. The whole available phase space is traced and longer integrations lead basically to the same shape. This shape does not correspond to a "typical" chaotic state, where the central limit theorem holds and the distributions can be fitted by a gaussian, since the correlations die out. Neither does it to an intermittent system, where the shape might be a combination of a normal density and a stretched exponential tail, due to the long correlation persistence.

As we are analyzing the evolution or stationarity of the distributions, it is important to keep in mind the difference between stationarity, due to the dynamics at certain time, and ergodicity, time-averaged property of the trajectories. In a non-ergodic orbit, the trajectory does not cover the whole hypersurface of constant energy, so two different initial conditions cover different parts of the energy surface leading to different temporal averages even for times tending to infinite. In such systems there is not a unique equilibrium state, but different ones depending on the starting point. Reversely, in an ergodic system it can be reached a unique equilibrium state. And generic ensembles of initial conditions will evolve towards a given distribution, time-independent or with little variability on long time-scales. One key point is the time involved in such evolution towards the final state. If the physical time scales are relevant and that time is too long for being realistic, those ensembles will not be able to be used as valid skeleton for the observed system behavior. So when computing distributions from a set of initial conditions, we need to be sure they are in the same domain of the Poincaré section. In that is the case, we get again the solid histogram of Fig. 3(b). By other hand, the stationarity of a distribution can be defined when the statistical parameters does not change with time, and this depends on the (variable) dynamics along the given

orbit. When computed the distribution from a single orbit, the morphology may depend on the initial point, when the total integration time is not large enough, as several transients of different behavior are found (see Ref. [9]).

In order to catch the behavior of the transient periods, we have computed distributions formed integrating just 10^3 time units (150-times the crossing time), which are described in Table I. Three of them appear in Fig. 3(b). The characteristic time on which the orbit forgets its previous degree of instability is small (low correlation time), as they are quite different. The standard deviation of the distributions σ gives a measure of the degree in which χ deviates from the mean, being a measure of the stability or variability of the values of χ along the orbit. The probability of getting a positive value for a finite-time Lyapunov exponent F_+ takes different values ranging from 0.4 up to 0.7 quite randomly, what indicates different behaviors, ordered at some stages, chaotic in others, as reflected in the shape of the distributions. For instance, the first transient shows two well separated peaks, like a period-2 orbit, while the third transient shows a multi-peaked distribution. When the time evolution of the finite-time Lyapunov distributions is compared with the way the consequents of the Poincaré section fill the available phase space, we see how each distribution corresponds to a different way of tracing the Poincaré section. If we change the interval size Δt by a small integer factor, our result is only a re-scaling of the spectrum, as was shown in Ref.[11]. However when it is increased up to, say, $\Delta t = 1$, which is still smaller than the averaged crossing time, a different multi-peaked shape is obtained, as shows the solid line in Fig. 4. The local details are washed up as the interval size is larger than the crossing time, so with a $\Delta t = 10$ (dotted line), the shape is again different. Now two main peaks well fitted by gaussians centered around positive values are observed. For even larger values of $\Delta t = 100$, a single peak gaussian distribution is found, since the central limit theorem begins to hold. Finally, for much larger values of $\Delta t = 100$, the distributions collapse to δ-functions centered around the global Lyapunov value. In addition, the chaoticity indicators vary with the interval size. The values in Table III are calculated as in Table I, but with $\Delta t = 1$. The mean value calculated with the larger interval on each transient is different to the calculated with the smallest interval. Moreover, the values of F_+ are larger, and for even larger interval sizes, the transients may vanish. Nevertheless it is remarkable that the evolution of F_+, which is an indicator of the local chaoticity, is similar in both cases. The Table II shows how the total integration time for a given interval size is correlated with

9

these indicators, showing that for the smallest interval we obtain similar results.

Finally, the characterization of the distributions corresponding to chaotic orbits is discussed. We take an orbit with an initial energy $E = 1/8$, that almost fills completely the available phase space, as shown by the Poincaré cross section in Fig. 5(a). The corresponding distribution is plotted in Fig. 5(b). The same distribution is obtained by integrating along a single initial condition or an ensemble of initial conditions, due to the ergodicity of the system. The shape reminds the one described for attractors in [20] and [15], although the tail of the peak centered around positive values extends through negative values quite smoothly, instead of showing an exponential tail. Two different transients of 10^3 time units are plotted as dotted and dashed lines in Fig. 5(b). We also see that the sticky orbits, those that remain near a regular island for a long time, tend to have smaller exponents than the non-sticky orbits. During the sticky periods, when the orbit appears next to a quasi-periodic orbit torus, the distribution is clearly similar to a quasi-periodic case. However, in the chaotic regime the peaks are broadened. With larger intervals ($\Delta t = 10$) and integration times (10^6 time units), an almost gaussian shaped distribution is obtained, centered around a positive value. This shows a morphology different from the $E = 1/12$ case, meaning a different dynamics, which is also manifested by the time the distribution takes to its final state.

III.   CONCLUSIONS

The results presented here are of general interest in describing how the distributions of finite-time Lyapunov exponents are valid indicators when computed with the smallest time interval. Several prototypical distribution morphologies have been plotted for different energy values of the Hénon-Heiles Hamiltonian. These calculations can be carried out in three ways. First, calculating a huge number N of short-time exponents of size Δt along the same orbit. Second, taking a smaller number of larger Δt (to allow the values to saturate). Third, selecting carefully an ensemble of N initial conditions in the same domain. Our calculations have focused in the use of the smallest interval size, searching for the stationarity or evolution of the distributions. It has been observed that they characterize the motion in the different possible cases. Shapes well differentiated from the ones described in the literature have been found. In the quasi-periodic case, the final shape is independent

of the initial point along the orbit and is reached after a small integration time (a few times the crossing time). For larger intervals, the shape is still well differentiated from the other cases, even when a short integration time is used. In the chaotic motions of energy values $E = 1/12$ and $E = 1/8$, the shape depends strongly on the initial point for short total integration times, since the distribution evolves through several transients and consequently several cycles are required before reaching the final shape. According to Ref. [5], the spectrum of chaotic orbits is invariant with respect to the initial conditions along the same invariant curve, but this only is applicable for large integrations or large intervals. However, tracing the distributions with the smallest intervals gives information on the local evolution of the chaoticity for short time scales. The morphology of the distributions traces the dynamics and the evolution of the value F_+ is the same independently of the interval size.

One interesting point is to analyze the sources of the components of the distribution morphology. The overall shape depends on the local orbit behavior, but this can be understood in terms of simplier periodic orbits, as possible basic blocks for shadowing the observed complicated behavior. This is a quite interesting reseach topic that can extend the current results, by studying the role of such periodic orbits in the building of the described structures.

As different parts of the same chaotic orbit may show different local exponents values in the different transients, this would indicate that the chaotic phase mixing [22] could be larger than the regular phase mixing at certain physical relevant time scales. We may conclude from here that different rates might exist in the evolution of the system towards its final state.

Our analysis has focused in a Hamiltonian system, where the stochastic orbits are ergodic. In this case, the results from generating the distributions from an adequate ensemble or from a single orbit are equivalent. But by taking the later approach, we were also able to manage with the distributions of non-ergodic orbits. The results obtained with this approach should be valid for orbits both in conservative or non-conservative systems, and in the case of dissipative systems, the distributions of the attractors described in the literature can be found. But as an evolution towards a final distribution is not guaranteed in a given time, the results on the stationarity or evolution during that period hold.

In addition, for bi-dimensional Hamiltonians as this one, the existence of KAM tori

produces the existence of sticky and non-sticky orbits, so the described phenomenology on the sticky transients is specific of this type of systems. It should be remarked that for tri-dimensional Hamiltonians, the cantori appear and this is no longer applicable as, in the end, the Arnold diffusion merge the orbits.

The previous discussion shows some implications from the physical meaning of the system. As the long integrations required for computing the global Lyapunov exponents have no meaning in a galactic system, since the universe evolves in a shorter time, it is reasonable to use smaller integrations. Furthermore, the smallest interval sizes can be used since they characterize the local behavior.

[1] H.E. Kandrup and M.E. Mahon, "Short Times Characterisations of Stochasticity in Noninte-grable Galactic Potentials", Astronomy and Astrophysics. 290 (1994) 762.

[2] M.E. Mahon, R.A. Abernathy, B.O. Bradley and H.E. Kandrup, "Transient ensemble dynamics in time-independent galactic potentials", Mon. Not. R. Astron. Soc. 275 (1995) 443.

[3] G. Contopoulos and N. Voglis, "A fast method for distinguishing between ordered and chaotic orbits", Astronomy and Astrophysics 317 (1997) 317

[4] K. Tsiganis, A. Anastasiadis and H. Varvoglis, "Dimensionality differences between sticky and non-sticky chaotic trajectory segments in a 3D Hamiltonian system", Chaos, Solitons & Fractals, (2000) 2281.

[5] G. Contopoulos, E. Grousousakou and N. Voglis, "Invariant spectra in Hamiltonian systems", Astronomy and Astrophysics 304 (1995) 374.

[6] A. Prasad and R. Ramaswany, "Characteristic distributions of finite-time Lyapunov exponents", Phys. Rev. E 60 (1999) 2761.

[7] F.K. Diakonos, D. Pingel and P. Schmelcher, "Analyzing Lyapunov Spectra of Chaotic Dynamical Systems", Phys. Rev. E 62 (2000) 4413.

[8] K. Alligood, T.D. Sauer and J.A. Yorke, Chaos. An Introduction to Dynamical Systems, Springer Verlag, New-York, 1996, p.383.

[9] C. Ziehmann, L. A. Smith and J. Kurths, "Localized Lyapunov exponents and the prediction of predictability", Phys. Let. A 271 (2000) 237

[10] P.A. Patsis, C. Efthymiopoulos, G. Contopoulos and N. Voglis, "Dynamical spectra of barred galaxies", Astron. Astrophys. 326 (1997) 493.

[11] H. Smith and G. Contopoulos, "Spectra of stretching numbers of orbits in oscillating galaxies", Astron. Astrophys. 314 (1996) 795.

[12] J.M. Finn, J.D. Hanson, I. Kan and E. Ott, "Steady fast dynamo flows", Phys. Fluids B 3 (1991) 1250.

[13] H. Yang, "Dependence of Hamiltonian Chaos on perturbation structure", International Journal Of Bifurcation and Chaos, 3 (1993) 1013.

[14] C. Siopis, H.E. Kandrup, G. Contopoulos and R. Dvorak, "Universal Properties of Escape in Dynamical Systems," Celestial Mechanics and Dynamical Astronomy 65 (1997) 57.

[15] A. Prasad and R. Ramaswamy, "Finite-time Lyapunov exponents of Strange Nonchaotic Attractors", in Nonlinear Dynamics: Integrability and Chaos, edited by M Daniel, R Sahadevan and K Tamizhmani (Narosa, New Delhi, 2000) pp. 227–34.

[16] R.L. Viana and C. Grebogi,"Unstable dimension variability and synchronization of chaotic systems", Phys. Rev. E 62 (2000) 462.

[17] H.R. Moser and P.F. Meier, "The structure of a Lyapunov spectrum can be determined locally", Phys. Let. A 263 (1999) 167.

[18] M. Hénon and C. Heiles,"The applicability of the third integral of motion: some numerical experiments", Astron. J. 69 (1964) 73.

[19] Y.-C. Lai, C. Grebogi and J.Kurths, "Modeling of deterministic chaotic systems", Phys. Rev E 59 (1999) 2907.

[20] E.J. Kostelich, I. Kan, C. Grebogi, E. Ott and J.A. Yorke, "Unstable Dimension Variability: A Source of Nonhyperbolicity in Chaotic Systems", Physica D 109 (1997) 81.

[21] J. Aguirre, J.C. Vallejo and M.A.F. Sanjuán, "Wada basins and chaotic invariant sets in the Hénon-Heiles system", Phys. Rev. E 64 (2001) 066208.

[22] H.E. Kandrup, "Phase Mixing in Time-Independent Hamiltonian Systems", Mon. Not. R. Astron. Soc. 301 (1998) 960.

[23] H.E. Nusse and J.A. Yorke, Dynamics: Numerical Explorations, Springer, New York, 1998, 2nd edition.
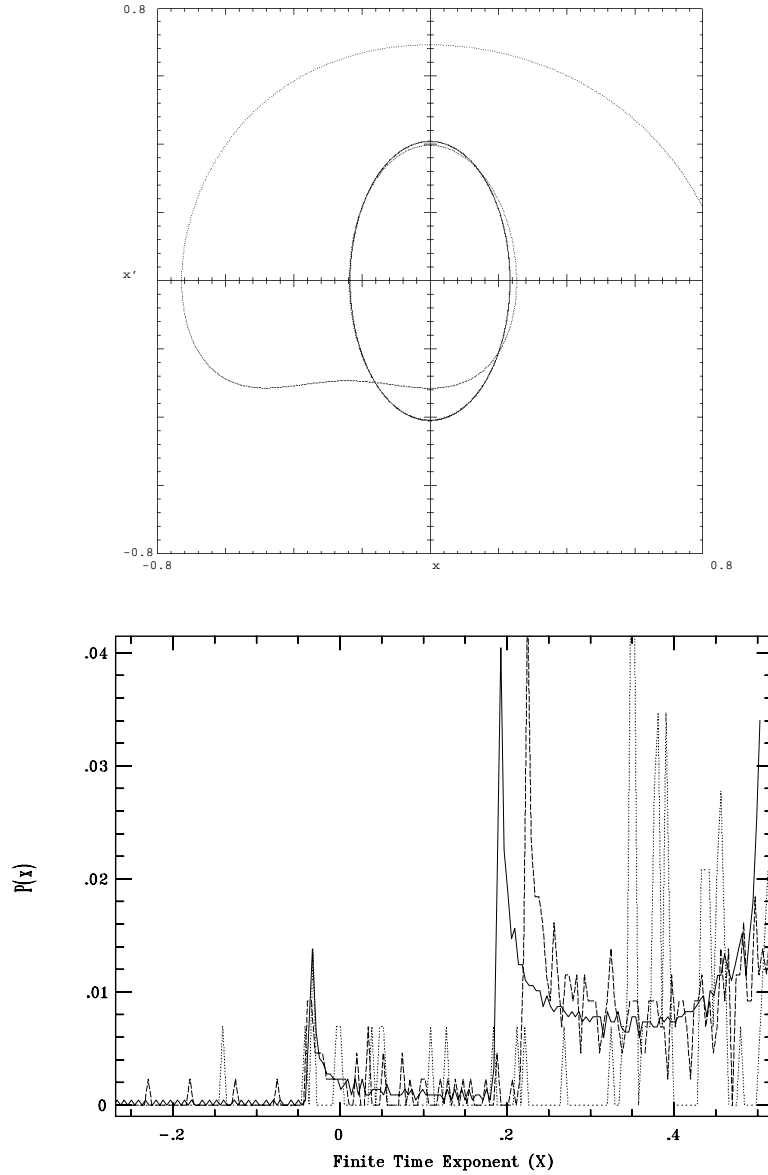
Fig. 1 VALLEJO, AGUIRRE & SANJUÁN

FIG. 1: (a) Orbit near an UPO, when $E = 1/4$. The period T is roughly 3.6 time units. (b) The solid line shows the distribution formed with an integration of 40 time-units when $\Delta t = 0.02$. The rightmost two peaks are traced when the orbit is confined, before escaping after $8T$ time-units. Dashed distribution is when $\Delta t = 0.1$ and dotted one when $\Delta t = 0.3$
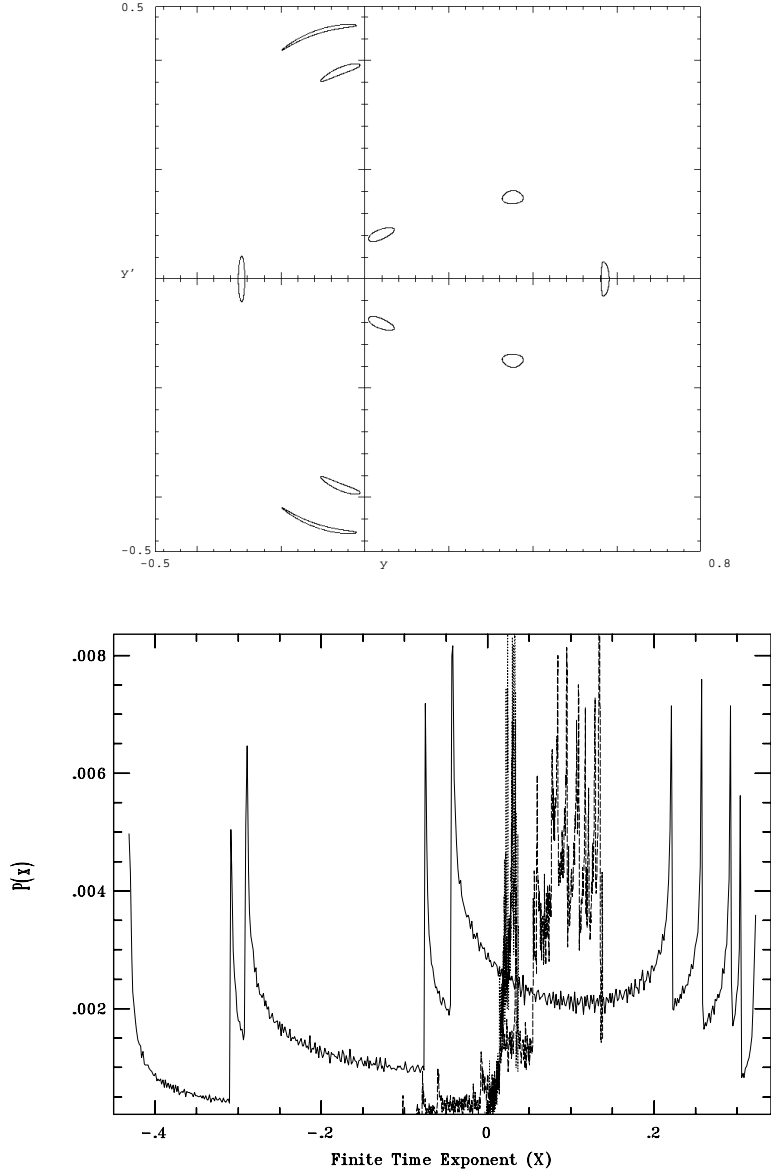
Fig. 2 VALLEJO, AGUIRRE & SANJUÁN

15

FIG. 2: (a) Poincaré cross-section of a quasi-periodic orbit of energy $E = 1/8$, associated to a period-5 orbit. The crossing time is aproximately 6.2 time units. Each time a point crosses the section, a different island is crossed and the total time before repeating an island is roughly 31.5 time units. (b) Distribution of finite-time Lyapunov exponents, showing 10 peaks both in positive and negative values, when $\Delta t = 0.02$ and total integration time 10^4 time units. The dashed distribution is when $\Delta t = 10$ and integration time 10^6. The dotted one is with $\Delta t = 100$ and integration time 10^6.
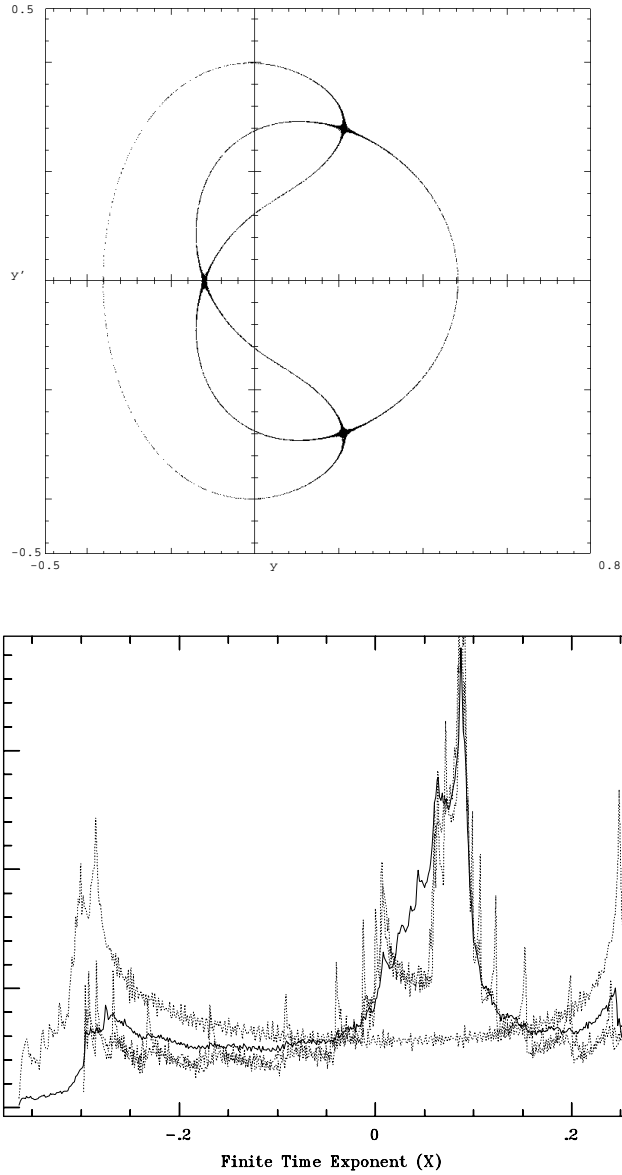
FIG. 3: (a) Poincaré cross-section of an orbit of energy $E = 1/12$. The crossing time is aproximately 6.75 time-units. (b) The solid line shows the distribution of finite-time Lyapunov exponents formed with an integration of 20000 time-units when $\Delta t = 0.02$. The dotted and dashed distributions corresponds to partial 1000 time-units integrations started at arbitrary points of the same orbit.

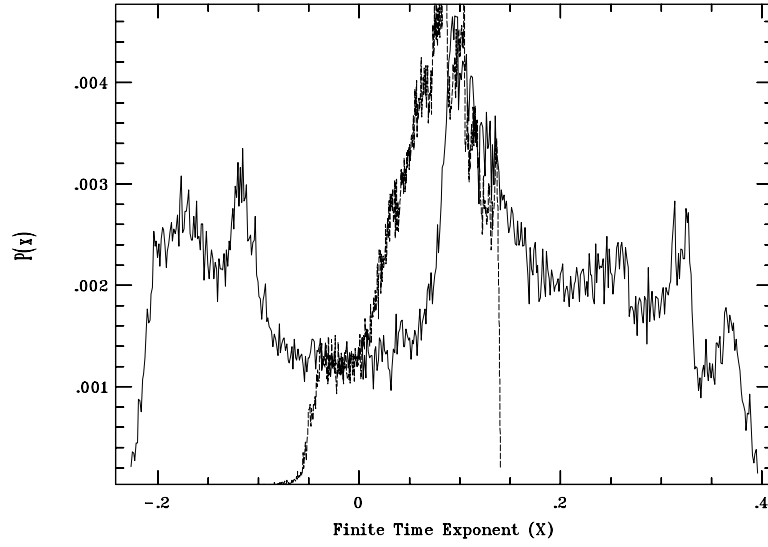**Fig. 3 VALLEJO, AGUIRRE & SANJUÁN**

17

FIG. 4: The distribution of finite-time Lyapunov exponents in the case $E = 1/12$ formed with an integration of 10^6 time units when $\Delta t = 1$ is plotted as solid trace. The same when $\Delta t = 10$ in dashed trace.
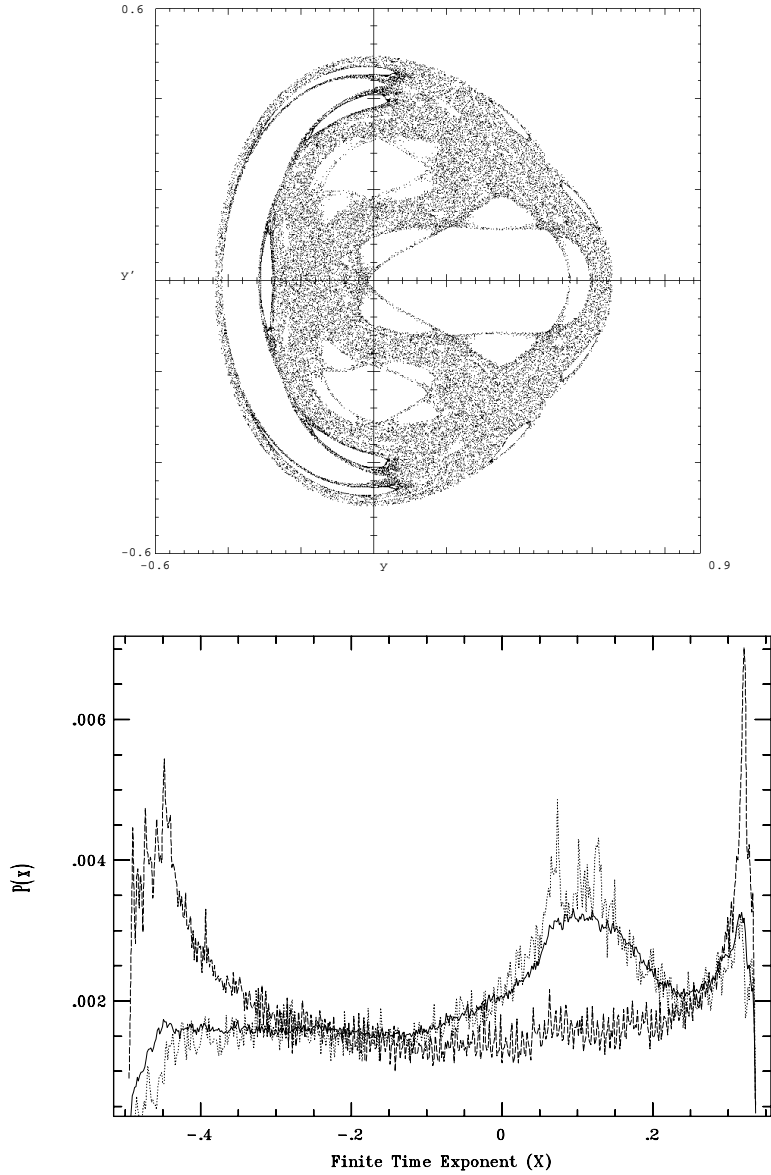
Fig. 4 VALLEJO, AGUIRRE & SANJUÁN

FIG. 5: (a) Poincaré cross-section of an orbit of energy $E = 1/8$. The crossing time is aproximately 6.80 time-units. (b) Distribution of finite-time Lyapunov exponents. The solid line corresponds to an integration of 20000 time-units when $\Delta t = 0.02$. The dotted and dashed ones to partial integrations of 10^3 time units. The double peaked one corresponds to a sticky period.

Fig. 5 VALLEJO, AGUIRRE & SANJUÁN

19

TABLE I: Several distribution behaviors in the case $E = 1/12$ for the smallest interval size $\Delta t = 0.02$. The statistics are for integrations of 10^3 time units starting at t_0.

t_0	Mean	Std. Dev.	Median	$F_+(t_0)$
0	-0.04402	0.18489	-0.44017	0.43455
10^3	-0.01337	0.16457	-0.01337	0.67674
$2 \cdot 10^3$	-0.01318	0.16437	-0.01318	0.66708
$3 \cdot 10^3$	-0.01318	0.16438	-0.01318	0.67882
$12 \cdot 10^3$	-0.04406	0.18492	-0.04406	0.47806
$14 \cdot 10^3$	-0.016346	0.152195	-0.016346	0.700080

Table I VALLEJO, AGUIRRE & SANJUÁN

TABLE II: Sensitivity of statistics of the finite-time Lypunov distributions in the case $E = 1/12$ for several integration time and interval sizes.

t(total time)	Δt(time)	Δt(steps)	Mean	Std. Dev.	Median	$F_+(t_0)$
$2 \cdot 10^4$	0.02	2	-0.04403	0.18490	-0.04403	0.64226
$2 \cdot 10^5$	0.02	2	-0.44069	0.18492	-0.04407	0.65772
$2 \cdot 10^4$	1	100	0.08553	0.17873	0.08553	0.69000
$2 \cdot 10^5$	1	100	0.08454	0.18004	0.08454	0.71060
$2 \cdot 10^4$	10	1000	0.032154	0.06258	0.32154	0.90400
$2 \cdot 10^5$	10	1000	0.02509	0.06671	0.02511	0.89565

Table II VALLEJO, AGUIRRE & SANJUÁN

TABLE III: Several distribution behaviors in the case $E = 1/12$ for interval size $\Delta t = 1$. The statistics are for integrations of 10^3 time units starting at t_0.

t_0	Mean	Std. Dev.	Median	$F_+(t_0)$
0	0.07362	0.17391	0.07362	0.46000
10^3	0.09552	0.17119	0.09552	0.74000
$2 \cdot 10^3$	0.09293	0.17478	0.09293	0.72000
$3 \cdot 10^3$	0.09117	0.17415	0.09117	0.73000
$12 \cdot 10^3$	0.06484	0.16613	0.06484	0.51000
$14 \cdot 10^3$	0.08573	0.14284	0.08573	0.75000

Table III VALLEJO, AGUIRRE & SANJUÁN